

Universal scaling for disordered viscoelastic matter I: Dynamic susceptibility at the onset of rigidity

Danilo B. Liarte,^{*} Stephen J. Thornton, Eric Schwen, Itai Cohen, Debanjan Chowdhury, and James P. Sethna
Department of Physics, Cornell University, Ithaca, NY 14853, USA

(Dated: March 1, 2025)

The onset of rigidity in interacting liquids, as they undergo a transition to a disordered solid, is associated with a dramatic rearrangement of the low-frequency vibrational spectrum. In this letter, we derive scaling forms for the singular dynamical response of disordered viscoelastic networks near both jamming and rigidity percolation. Using effective-medium theory, we extract critical exponents, invariant scaling combinations and analytical formulas for universal scaling functions near these transitions. Our scaling forms describe the behavior in space and time near the various onsets of rigidity, for rigid and floppy phases and the crossover region, including diverging length and time scales at the transitions. We expect that these behaviors can be measured in systems ranging from colloidal suspensions to anomalous charge-density fluctuations of “strange” metals.

Jamming [1] and *Rigid Percolation* (RP) [2] provide suitable frameworks to characterize the fascinating invariant scaling behavior exhibited by several classes of disordered viscoelastic materials near the onset of rigidity [3]. Both are often described by elastic networks near the Maxwell limit of mechanical stability [4], and represent transitions from a rigid phase to a floppy one when the average coordination number z falls below the isostatic value z_c . RP appears in network glasses [5], fiber networks [6, 7] and soft colloidal gels [8], and is described in terms of networks in which bonds are randomly removed; the bulk modulus vanishes [9] at the transition [10–12]. Jamming is also a ubiquitous phenomenon arising in systems ranging from amorphous solids and glasses [13] to cell tissues [14] and deep learning [15]. Jamming is commonly described in terms of sphere packings that possess a finite bulk modulus $B > 0$ at the transition. Recently, it was shown that jamming can be described as a multi-critical point that terminates a line of continuous transitions associated with rigidity percolation and that there is a deep connection between the universal scaling forms for both transitions [16]. Determining explicit formulas for the susceptibilities and space-time correlations has been challenging, however, since there is a scarcity both of comprehensive numerical data and of analytic models for these transitions (with the exception of jamming in high dimensions [17–19]). Here, we leverage the analytically-tractable effective-medium theory (EMT) of Ref. [16] to fill this gap and extract explicit equations for these universal forms.

At jamming [1], two-dimensional disk packings form a disordered contact network [blue lines in Fig. 1(a)] that supports compression but not shear. Mimicking compression by randomly adding next-nearest neighbor bonds between disks [red N-bonds in Fig. 1(a)] and/or randomly removing B-bonds can lead to either jamming or RP depending on the population for each type of bond [16]. A simpler model that yields the same scaling behavior consists of randomly placing ‘B’ and ‘N’-bonds between nearest and next-nearest neighbor pairs of sites [blue and red

solid lines in Fig. 1(b)] of a periodic honeycomb lattice. This network describes a diluted version of a 3-sub-lattice system consisting of a honeycomb lattice [shaded blue in Fig. 1(b)] and two triangular lattices (shaded red; here we show only the bonds of one triangular lattice). Detailed knowledge of the mechanical behavior of periodic lattices allowed the development of an EMT at finite dimension [20] for jamming [16] and for the crossover from jamming to RP, valid in both rigid and floppy states. We will employ these results to derive *explicit solutions* for the critical scaling of the susceptibilities of disordered viscoelastic matter near jamming and RP. Our analysis not only allows for quick assessment of scale-invariant behavior of quantities such as viscosities and correlations (without the need for computationally-expensive simulations); it also serves as an example of how one may analyze rigidity transitions for which the universality class has not been determined.

Figure 1(c) shows the phase diagram of the honeycomb-triangular lattice (HTL) model in terms of occupation probability of nearest neighbor B bonds and next-nearest neighbor N bonds. Rigid (yellow) and floppy regions are separated by an RP line that terminates in a multicritical jamming point J (red disk). From Fig. 1(c), one can also extract definitions for the scaling variables δ_J and δ_{RP} , chosen so that $\delta_{RP} = 0$ at RP, and δ_J is also zero at jamming.

RP should generically be codimension one, because only one constraint (isostaticity) needs to be satisfied. In the HTL model of Fig. 1(b), jamming is codimension two. But the jump in bulk modulus characteristic of jamming here demands a complete honeycomb lattice; one can see that if the three orientations of hexagon bonds were independently populated, the jamming transition would be codimension four (their three probabilities set to one plus isostaticity). This special tuning of the system to favor the bulk modulus is echoed in the jamming of frictionless spheres, where the first state of self stress [21] leads to a jump in the bulk modulus because the conjugate degree of freedom (a uniform compression) was used to

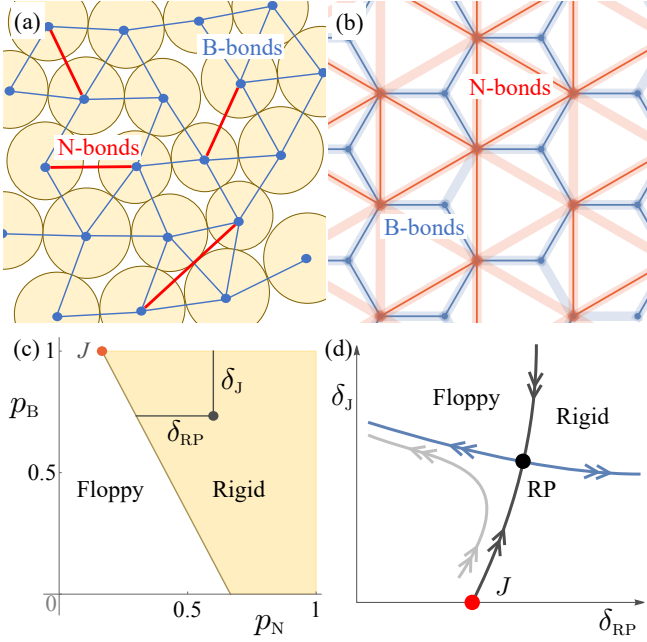


FIG. 1. (a) Jammed disk packing, underlying contact network (B-bonds in blue) and randomly added next-nearest neighbor N-bonds (red). (b) HTL model with nearest and next-nearest neighbor bonds (solid blue and red lines) connecting sites of a honeycomb and triangular lattices, respectively. (c) Phase diagram of the HTL model in terms of occupation probabilities for B and N-bonds. The yellow region corresponds to the rigid state, and is separated from the floppy state by an RP line ending at a jamming point J (red disk). (d) Conjecture for a crossover flow diagram projected into $\delta_{RP} \times \delta_J$ space. J (red disk) and RP (black disk) represent fixed points of a putative renormalization-group scheme. The blue, black and gray lines represent the unstable manifold, the critical line and a sample trajectory, respectively.

tune the system to the rigidity transition. As evidence for this, shear jamming of frictionless spheres has a jump in a single anisotropic modulus [22].

We conjecture that there is a class of disordered elastic systems for which a renormalization-group scheme leads to the typical crossover flow diagram [23] (projected in $\delta_{RP} \times \delta_J$ space) illustrated in Fig. 1(d). The scaling variable $\delta_{RP} \propto \Delta z \equiv z - z_c$ must be relevant for both jamming and RP, but the depletion probability of the B-lattice δ_J is relevant only for jamming. This behavior is captured by the direction of the arrows coming in and out of the putative jamming and RP fixed points (red and black disks, respectively) in Fig. 1(d). A system near the J fixed point ($\delta_J, |\delta_{RP}| \ll 1$) will be controlled either by J if a crossover variable $\delta_J/|\delta_{RP}|^\varphi \ll 1$ for some exponent φ , or by RP if $\delta_J/|\delta_{RP}|^\varphi \gg 1$, i.e. for trajectories such as the gray line passing sufficiently close to the critical line (black solid line.) Though δ_J does not have a direct interpretation in the jamming of sphere packings [except for

the network model of Fig. 1(a)], there might be variables that play a similar role, such as attractive interactions in soft gels [24].

We now introduce a scaling *ansatz* for the longitudinal response function [25] near jamming:

$$\frac{\chi_L}{\chi_0} \approx |\delta_{RP}|^{-\gamma} \mathcal{L} \left(\frac{q/q_0}{|\delta_{RP}|^\nu}, \frac{\omega/\omega_0}{|\delta_{RP}|^{z\nu}}, \frac{\delta_J/\delta_0}{|\delta_{RP}|^\varphi} \right), \quad (1)$$

where q is the wavevector, ω is the frequency, γ , ν , z and φ are critical exponents for the susceptibility, correlation length, correlation time, and crossover behavior, respectively [23, 26], and \mathcal{L} is a universal scaling function. The constants χ_0 , q_0 , ω_0 and δ_0 are nonuniversal scaling factors. Many other properties can be derived from \mathcal{L} (Table II). Such space-time susceptibilities, and the corresponding structure and correlation functions, are the fundamental linear response quantities for materials. They have been well studied in glassy systems, but have hitherto not been a focus in the study of jamming or RP. Baumgarten et al. [27] and Hexner et al. [28] have studied the static response of frictionless jammed spheres to a sinusoidal perturbation; they find diverging length scales that are different from the ones presented here. Because our system is on a regular lattice, and particularly because our analysis replaces the disordered lattice with a uniform one, it is natural for us to fill this gap.

Our approach goes beyond previous work [29] in two aspects. First, rather than starting with an ansatz for the free energy in terms of the excess contact number Δz , excess packing fraction $\Delta\phi$, shear stress ϵ and system size N , we consider the longitudinal response in terms of δ_{RP} , q , ω and δ_J . Our variable δ_{RP} is proportional to Δz . Though we do not consider an explicit dependence of χ_L on ϵ or $\Delta\phi$ [30], we can extract equivalent expressions for moduli and correlations from the dependence of χ_L on q . Importantly, the inclusion of ω in our analysis allows us to predict dynamical properties such as viscosities.

Second, we use EMT [16] to derive and validate both the universal exponents and the universal scaling functions (\mathcal{L}), for both jamming and RP. This form of EMT is based on the coherent-potential approximation [10, 31] (CPA), and is known to reproduce well results obtained from simulations of randomly-diluted lattices with two-body [32] harmonic interactions [33, 34], even for undamped [11, 16] and overdamped dynamics [35, 36]. Although the CPA involves mean-field-like uncontrolled approximations, it preserves the topology of the original lattices — an essential ingredient that ultimately allows one to describe jamming. Here we focus on the longitudinal response, since the full response of isotropic elastic systems can be decomposed into longitudinal and transverse components, and the latter has the same scaling form near both jamming and RP as the longitudinal response near RP; see [37].

We use the long wavelength limit of the longitudinal response χ_L along with EMT results from Ref. [16] to

derive critical exponents (see Table I) and the universal scaling function \mathcal{L} in Eq. (1) (see [37]),

$$\mathcal{L}(u, v, w) = \left[\frac{u^2}{1 + w / (\sqrt{1 - \tilde{v}(v)} \pm 1)} - \tilde{v}(v) \right]^{-1}, \quad (2)$$

where $\tilde{v}(v) = v^2$ and $i v$ for undamped and overdamped dynamics, respectively, and the plus and minus signs correspond to solutions in the elastic and floppy states, respectively. Equation (2) embodies the central results of this paper. From Eqs. (1) and (2), we will extract the universal behavior of the elastic moduli, viscosities as well as the density response and correlation functions (dynamic structure factor). Though it is not certain that these functions are as universal as critical exponents, recent simulations of compressed hyper-spheres [38] indicate that critical amplitudes calculated using mean-field models at infinite dimension are preserved for low-dimensional jammed packings.

	γ	z	ν	φ	β_B	γ_B
Jamming	2	1 (2)	1	1	0	1 (2)
Rigidity Percolation	2	2 (4)	1/2	-	1	0 (1)

TABLE I. Critical exponents for the longitudinal susceptibility (γ), correlation length (ν), correlation time (z) and crossover behavior (φ) near jamming and RP for undamped and overdamped (between parentheses if different from undamped) dynamics. The exponents β_B and γ_B can be derived from γ , ν and z (see Table II), and describe power-law singularities for the bulk modulus and viscosity, respectively.

For $|\delta_{RP}| \ll \delta_J$ [$w \gg 1$ in Eq. (2)], our model exhibits RP criticality: δ_J becomes an irrelevant variable, and $\mathcal{L}(u, v, w) \rightarrow \tilde{\mathcal{L}}(u, v)$, with

$$\tilde{\mathcal{L}}(u, v) = \left[u^2 \left(\sqrt{1 - \tilde{v}(v)} \pm 1 \right) - \tilde{v}(v) \right]^{-1}. \quad (3)$$

Here the change in \mathcal{L} is accompanied by a change in the critical exponents ν and z (see Table I). Note that the invariant scaling combinations $q/|\delta_{RP}|^\nu$ and $\omega/|\delta_{RP}|^{z\nu}$ lead to definitions for diverging length and time scales, $\ell \sim 1/|\delta_{RP}|^\nu$ and $\tau \sim 1/|\delta_{RP}|^{z\nu}$, respectively. The exponent $z\nu$ depends only on the type of dynamics, but the exponent ν (equals 1 and 1/2 for jamming and RP, respectively) emerges naturally in our approach and is consistent with more elaborate definitions involving cutting boundaries [13].

Scale invariance, as captured by Eqs. (1) and (2), implies that the relation between rescaled versions of χ_L , q , ω and δ_J does not depend on δ_{RP} . To validate this result, we show in Figs. 2(a) and (b) *scaling collapse plots* of the longitudinal response as a function of the frequency scaling combination $v = (\omega/\omega_0)/|\delta_{RP}|^{z\nu}$, near jamming and RP, for overdamped dynamics in the rigid phase. Real

parts are in blue; imaginary (dissipative) parts in red. The solid and dashed curves are the asymptotic universal scaling predictions [Eqs. (2) and (3)] at two different values of the wavevector scaling variable $q/|\delta_{RP}|^\nu$. Symbols clearly converge to our universal scaling forms, and are full solutions of the EMT equations for several values of δ_{RP} , along paths approaching jamming and RP. We approach the jamming point at constant $\delta_J/|\delta_{RP}|^\varphi$.

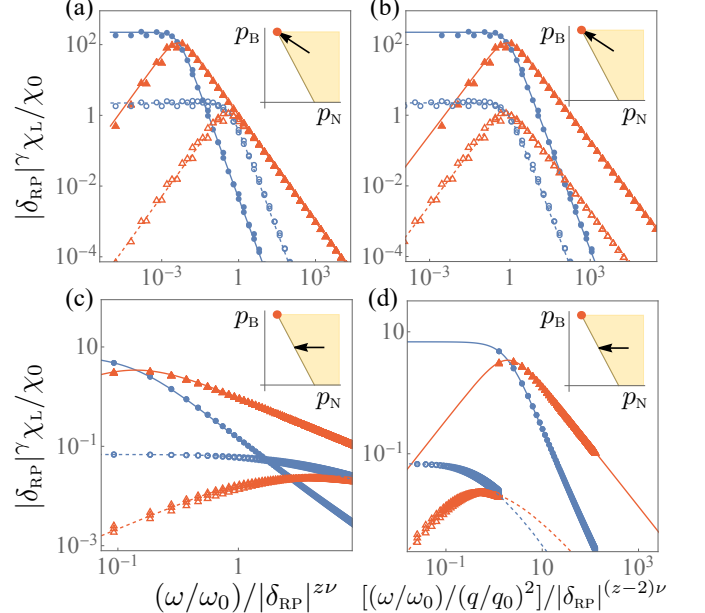


FIG. 2. Scaling collapse of the longitudinal response near jamming and RP for overdamped dynamics following the paths indicated by arrows in the inset of each panel [cf. Fig. 1(c)]. Blue disks and red triangles correspond to full solutions of the EMT equations for the real and imaginary parts of $|\delta_{RP}|^\gamma \chi_L$, respectively. Solid and dashed curves correspond to the universal scaling predictions of Eqs. (2) and (3). Dashed [solid] lines correspond to $q/|\delta_{RP}|^\nu = 1$ [0.1]. We approach the jamming point along $\delta_J/|\delta_{RP}|^\varphi$ equal to $\sqrt{5}/4$ from the rigid side. Full solutions run at $|\delta_{RP}| = 10^{-2}$, 10^{-3} , and 10^{-4} for RP and a range $|\delta_{RP}| \in [5 \times 10^{-2}, 5 \times 10^{-6}]$ for jamming show convergence to our universal asymptotic predictions.

The collapses of Fig. 2 not only validate our universal scaling forms; they indicate an interesting crossover behavior of the complex response of disordered solids. Note that the real part $\mathcal{L}'(v)$ plateaus and the imaginary part $\mathcal{L}''(v)$ (the dissipation) vanishes at low frequency v . At high frequency, both \mathcal{L}' and \mathcal{L}'' decay to zero, but \mathcal{L}' decays faster than \mathcal{L}'' [39]. Hence, there is a frequency above which the response is dominated by the dissipative imaginary part, which scales as $D^* q^2$, where $D^* \sim |\delta_{RP}|^{(z-2)\nu}$ is a characteristic diffusion constant. To visualize this crossover at the ‘diffusion limit’, we plot in Figs. 2(b) and (d) the same data shown in Figs. 2(a) and (b), respectively, with the horizontal axis replaced by $v/u^2 \propto (\omega/q^2)/D^*$. Interestingly, although jamming

and RP exhibit the same qualitative behavior in terms of rescaled quantities, the exponent $(z-2)\nu$ of D^* is equal to zero for jamming and one for RP.

Equations (1) and (2) determine the scaling behavior of several quantities characterized by the general form,

$$\frac{Y}{Y_0} = |\delta_{\text{RP}}|^y \mathcal{Y} \left(\frac{q/q_0}{|\delta_{\text{RP}}|^\nu}, \frac{\omega/\omega_0}{|\delta_{\text{RP}}|^{z\nu}}, \frac{\delta_j/\delta_0}{|\delta_{\text{RP}}|^\varphi} \right), \quad (4)$$

where in Table II we present explicit expressions for the exponent y and universal function \mathcal{Y} describing the bulk modulus (B), viscosity (ζ), density response (Π) and correlation function (S). The behavior near RP is obtained by replacing \mathcal{Y} and \mathcal{L} in the third column of Table II by $\bar{\mathcal{Y}}$ and $\bar{\mathcal{L}}$ (now functions of u and v only), respectively, along with appropriate changes for the exponents (see Table I). The scaling behavior of the shear modulus and viscosity near jamming and RP is the same as that of B and ζ , respectively, near RP.

Y	y	\mathcal{Y}
B	$\beta_B \equiv \gamma - 2\nu$	$\mathcal{B} = (\partial \mathcal{L}^{-1} / \partial u) / (2u)$
ζ	$-\gamma_B \equiv \gamma - (2+z)\nu$	$\mathcal{Z} = (1/v) \text{Im}[\mathcal{B}]$
Π	$2\nu - \gamma$	$\mathcal{P} = u^2 \mathcal{L}$
S	$(2+z)\nu - \gamma$	$\mathcal{S} = (1/v) \text{Im}[\mathcal{P}]$

TABLE II. Critical exponent y and universal scaling function \mathcal{Y} describing the singular behavior of the bulk modulus B and viscosity ζ , density response Π and correlation function S , according to Eq. (4).

To illustrate the broad applicability of our scaling forms, we discuss our results for the density-density correlation — the structure function for isotropic fluids at $q \neq 0$. Figure 3(a) shows a 3D plot of the universal function $\bar{\mathcal{S}}(u, v)$ (see Table II) for undamped fluids near RP. At fixed u , $\bar{\mathcal{S}}(u, v)$ has a maximum (blue dashed line) at $v = v^* \approx \mathcal{O}(1)$ [i.e. $\omega^* \propto \delta_{\text{RP}}$] (see [37]), which coincides with the crossover from Debye to isostatic behavior, interpreted as the paradigmatic *boson peak* [40–42] of glasses [43]. Near jamming or RP, this point marks the onset of the enhancement of the population of low-energy modes [44] leading to a flat density of states at low frequency [16, 44]. At fixed v , $\bar{\mathcal{S}}$ plateaus at a value of u of $\mathcal{O}(1)$ (i.e. at $q \propto |\delta_{\text{RP}}|^{1/2}$). Our explicit formulas also provide a simple tool to map the global behavior of many quantities of interest. For example, Fig. 3(b) shows a diagram in terms of rescaled wavevector u and frequency v marking the boson peak (blue-dashed line) and regions where $\bar{\mathcal{S}}(u, v)$ exhibits power-law behavior. The blue region indicates the neighborhood of the boson peak, in which $\bar{\mathcal{S}}(u, v) > \bar{\mathcal{S}}(u, v^*)/2$, and the red and yellow regions show power-law regimes in u and v .

In this letter, we have combined scaling theory and the EMT of Ref. [16] to produce analytical formulas for

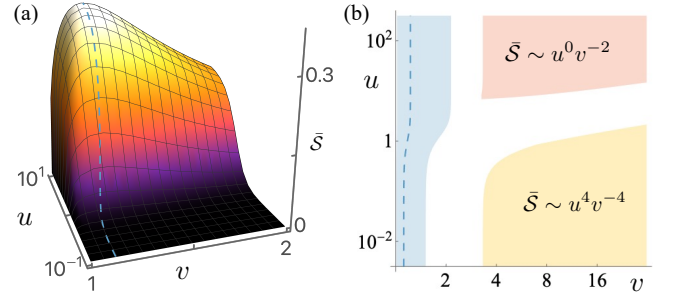


FIG. 3. (a) 3D plot of the universal scaling function for the correlation function $\bar{\mathcal{S}}(u, v)$, for undamped fluids near RP. The blue dashed line corresponds to the rescaled frequency v^* (the boson peak) at which $\bar{\mathcal{S}}(u, v)$ is maximum for fixed rescaled wavevector u . (b) $u \times v$ diagram showing the boson peak (blue dashed line) and power law regions for which $\bar{\mathcal{S}}(u, v) \propto u^\alpha v^\beta$, with (α, β) close to their asymptotic values $(0, -2)$ (red) and $(4, -4)$ (yellow). In the blue region the condition $\bar{\mathcal{S}}(u, v) > \bar{\mathcal{S}}(u, v^*)/2$ is satisfied.

universal scaling functions for the longitudinal dynamical response near both jamming and RP. Our equations can be used to determine the space-time dependence of universal functions for several quantities (such as moduli, viscosities and correlations) near the onset of rigidity in both the solid and liquid phases. A direct approach to experimentally validate our predictions consists of using 3D printers to fabricate and perform experiments on the disordered elastic networks illustrated in Figs. 1(a) and (b). We also expect these scaling forms to apply to more traditional glass forming systems such as colloidal suspensions. Here, in addition to more standard scattering measurements, new techniques for measuring 3D particle positions and even stresses with high precision may make it feasible to measure these functional forms and test our predictions [45–48]. In such suspensions, we expect that the scaling functions will capture the behavior in the elastic regime. However, our theory is built on a fixed network topology and lacks some features of the liquid phase. Annealed rather than quenched disorder [23] (or even intermediate disorder [49]) could be needed to describe viscoelastic fluids. An extension of our analysis includes an investigation [50] of the intriguing connections between the featureless low-energy modes in our system and the unconventional *particle-hole continuum* measured using momentum and energy-resolved spectroscopic probes in certain *strange metals* [51, 52]. Other extensions could include the incorporation of *anisotropic* bond occupation [53], which plays a major role in the crossover scaling of thickening suspensions near frictional jamming [54] and that can lead to simpler models for both shear jamming [55] and thickening [56], as well as the incorporation of random stress fields, which can elucidate the unjamming of colloidal suspensions (such as titanium dioxide) due to activity [57].

We thank Andrea Liu, Bulbul Chakraborty, Daniel Hexner, Eleni Katifori, Emanuela del Gado, Itay Griniasty, Matthieu Wyart, Meera Ramaswamy, Peter Abamonte, Sean Ridout, Tom Lubensky and Xiaoming Mao for useful conversations. This work was supported in part by NSF DMR-1719490 (SJT and JPS), NSF CBET Award # 2010118 (DBL, ES, JPS, and IC) and NSF CBET Award # 1509308 (ES and IC). DBL also thanks ICTP-SAIFR for partial financial support through FAPESP grant # 2016/01343-7. DC is supported by a faculty startup grant at Cornell University.

* liarte@cornell.edu

- [1] A. J. Liu and S. R. Nagel, *Annual Review of Condensed Matter Physics* **1**, 347 (2010), <https://doi.org/10.1146/annurev-conmatphys-070909-104045>.
- [2] M. Thorpe, *Journal of Non-Crystalline Solids* **57**, 355 (1983).
- [3] J. P. Sethna, M. K. Bierbaum, K. A. Dahmen, C. P. Goodrich, J. R. Greer, L. X. Hayden, J. P. Kent-Dobias, E. D. Lee, D. B. Liarte, X. Ni, K. N. Quinn, A. Raju, D. Z. Rocklin, A. Shekhawat, and S. Zapperi, *Annual Review of Materials Research* **47**, 217 (2017).
- [4] J. C. M. F.R.S., *The London, Edinburgh, and Dublin Philosophical Magazine and Journal of Science* **27**, 294 (1864), <https://doi.org/10.1080/14786446408643668>.
- [5] M. Thorpe, D. Jacobs, N. Chubynsky, and A. Rader, “Generic rigidity of network glasses,” in *Rigidity Theory and Applications*, edited by M. F. Thorpe and P. M. Duxbury (Springer US, Boston, MA, 2002) pp. 239–277.
- [6] R. C. Picu, *Soft Matter* **7**, 6768 (2011).
- [7] C. P. Broedersz, X. Mao, T. C. Lubensky, and F. C. MacKintosh, *Nature Physics* **7**, 983 (2011).
- [8] S. Zhang, L. Zhang, M. Bouzid, D. Z. Rocklin, E. Del Gado, and X. Mao, *Phys. Rev. Lett.* **123**, 058001 (2019).
- [9] Different types of lattices do not *appear* to have the same universal RP behavior. For instance, isotropic periodic Maxwell lattices (in which $z = z_c = 2D$ where D is the dimension) can have $B, G > 0$ (as in the kagome lattice), where G is the shear modulus, or $B = 0$ and $G > 0$ (as in the twisted-kagome lattice, see e.g. [34]), which suggests that these lattices do not belong to the same RP universality class. However, if these lattices have extra bonds so that $z > 2D$, arbitrary protocols to randomly dilute these networks without specifically targeting particular bonds will lead to a continuous transition for both B and G .
- [10] S. Feng, M. F. Thorpe, and E. Garboczi, *Physical Review B* **31**, 276 (1985).
- [11] X. Mao and T. C. Lubensky, *Phys. Rev. E* **83**, 011111 (2011).
- [12] D. B. Liarte, O. Stenull, X. M. Mao, and T. C. Lubensky, *Journal of Physics-Condensed Matter* **28**, 165402 (2016).
- [13] A. J. Liu, S. R. Nagel, W. Van Saarloos, and M. Wyart, *Dynamical heterogeneities in glasses, colloids, and granular media*, 298 (2011).
- [14] D. Bi, X. Yang, M. C. Marchetti, and M. L. Manning, *Phys. Rev. X* **6**, 021011 (2016).
- [15] Y. Bahri, J. Kadmon, J. Pennington, S. S. Schoenholz, J. Sohl-Dickstein, and S. Ganguli, *Annual Review of Condensed Matter Physics* **11**, 501 (2020), <https://doi.org/10.1146/annurev-conmatphys-031119-050745>.
- [16] D. B. Liarte, X. Mao, O. Stenull, and T. C. Lubensky, *Phys. Rev. Lett.* **122**, 128006 (2019).
- [17] J. Kurchan, G. Parisi, and F. Zamponi, *Journal of Statistical Mechanics: Theory and Experiment* **2012**, P10012 (2012).
- [18] J. Kurchan, G. Parisi, P. Urbani, and F. Zamponi, *The Journal of Physical Chemistry B* **117**, 12979 (2013), pMID: 23581562, <https://doi.org/10.1021/jp402235d>.
- [19] P. Charbonneau, J. Kurchan, G. Parisi, P. Urbani, and F. Zamponi, *Journal of Statistical Mechanics: Theory and Experiment* **2014**, P10009 (2014).
- [20] See also Refs. [? ? ?] for calculations in finite dimension based on the nonaffine response of amorphous solids.
- [21] T. C. Lubensky, C. L. Kane, X. Mao, A. Souslov, and K. Sun, *Reports on Progress in Physics* **78**, 073901 (2015).
- [22] M. Baity-Jesi, C. P. Goodrich, A. J. Liu, S. R. Nagel, and J. P. Sethna, *Journal of Statistical Physics* **167**, 735 (2017).
- [23] J. Cardy, *Scaling and renormalization in statistical physics* (Cambridge university press, 1996).
- [24] E. del Gado and X. Mao, personal communication (2020).
- [25] P. Chaikin and T. Lubensky, *Principles of Condensed Matter Physics* (Cambridge University Press, Cambridge, 1995).
- [26] J. Sethna, *Statistical mechanics: entropy, order parameters, and complexity* (Oxford University Press, 2006).
- [27] K. Baumgarten, D. Vågberg, and B. P. Tighe, *Phys. Rev. Lett.* **118**, 098001 (2017).
- [28] D. Hexner, S. R. Nagel, and A. J. Liu, “The length dependent elasticity for jammed systems,” Poster presented at CECAM workshop, *Recent Advances on the Glass and Jamming Transitions*, (2017).
- [29] C. P. Goodrich, A. J. Liu, and J. P. Sethna, *Proceedings of the National Academy of Sciences* **113**, 9745 (2016), <https://www.pnas.org/content/113/35/9745.full.pdf>.
- [30] Note that δ_{RP} does not change with lattice deformation for our system. This contrasts with the case of compressed disks in which Δz can vary with $\Delta\phi$. We assume fixed (quenched) disorder in our model.
- [31] R. J. Elliott, J. A. Krumhansl, and P. L. Leath, *Rev. Mod. Phys.* **46**, 465 (1974).
- [32] A more sophisticated version of EMT is needed to reproduce the scaling behavior of randomly-diluted lattices with three-body forces such as bending [12].
- [33] L. M. Schwartz, S. Feng, M. F. Thorpe, and P. N. Sen, *Phys. Rev. B* **32**, 4607 (1985).
- [34] D. B. Liarte, O. Stenull, and T. C. Lubensky, *Phys. Rev. E* **101**, 063001 (2020).
- [35] M. G. Yucht, M. Sheinman, and C. P. Broedersz, *Soft Matter* **9**, 7000 (2013).
- [36] G. Duering, E. Lerner, and M. Wyart, *Soft Matter* **9**, 146 (2013).
- [37] D. B. Liarte, S. J. Thornton, E. Schwen, I. Cohen, D. Chowdhury, and J. P. Sethna, “Universal scaling for disordered viscoelastic matter ii: Collapses, global behavior and spatio-temporal properties,” (2022), [arXiv:2202.13933 \[cond-mat.soft\]](https://arxiv.org/abs/2202.13933).

- [38] J. D. Sartor, S. A. Ridout, and E. I. Corwin, *Phys. Rev. Lett.* **126**, 048001 (2021).
- [39] This is true except in the limit of very large u and v , where both \mathcal{L}' and \mathcal{L}'' decay as $v^{-1/2}$. See [37] for details.
- [40] V. Vitelli, N. Xu, M. Wyart, A. J. Liu, and S. R. Nagel, *Phys. Rev. E* **81**, 021301 (2010).
- [41] E. DeGiuli, A. Laversanne-Finot, G. Düring, E. Lerner, and M. Wyart, *Soft Matter* **10**, 5628 (2014).
- [42] S. Franz, G. Parisi, P. Urbani, and F. Zamponi, *Proceedings of the National Academy of Sciences* **112**, 14539 (2015), <https://www.pnas.org/content/112/47/14539.full.pdf>.
- [43] K. Binder and W. Kob, *Glassy materials and disordered solids: An introduction to their statistical mechanics* (World scientific, 2011).
- [44] L. E. Silbert, A. J. Liu, and S. R. Nagel, *Phys. Rev. Lett.* **95**, 098301 (2005).
- [45] E. R. Weeks, J. C. Crocker, A. C. Levitt, A. Schofield, and D. A. Weitz, *Science* **287**, 627 (2000).
- [46] N. Y. Lin, M. Bierbaum, P. Schall, J. P. Sethna, and I. Cohen, *Nature materials* **15**, 1172 (2016).
- [47] M. Bierbaum, B. D. Leahy, A. A. Alemi, I. Cohen, and J. P. Sethna, *Phys. Rev. X* **7**, 041007 (2017).
- [48] B. D. Leahy, N. Y. Lin, and I. Cohen, *Current Opinion in Colloid & Interface Science* **34**, 32 (2018).
- [49] E. do Carmo, D. B. Liarte, and S. R. Salinas, *Phys. Rev. E* **81**, 062701 (2010).
- [50] S. J. Thornton, D. B. Liarte, P. Abbamonte, J. P. Sethna, and D. Chowdhury, “Jamming and unusual charge density fluctuations of strange metals,” (2022), in preparation.
- [51] M. Mitrano, A. A. Husain, S. Vig, A. Kogar, M. S. Rak, S. I. Rubeck, J. Schmalian, B. Uchoa, J. Schneeloch, R. Zhong, G. D. Gu, and P. Abbamonte, *Proceedings of the National Academy of Sciences* **115**, 5392 (2018), <https://www.pnas.org/content/115/21/5392.full.pdf>.
- [52] A. A. Husain, M. Mitrano, M. S. Rak, S. Rubeck, B. Uchoa, K. March, C. Dwyer, J. Schneeloch, R. Zhong, G. D. Gu, and P. Abbamonte, *Phys. Rev. X* **9**, 041062 (2019).
- [53] T. Zhang, J. M. Schwarz, and M. Das, *Phys. Rev. E* **90**, 062139 (2014).
- [54] M. Ramaswamy, I. Griniasty, D. B. Liarte, A. Shetty, E. Katifori, E. D. Gado, J. P. Sethna, B. Chakraborty, and I. Cohen, “Universal scaling of shear thickening transitions,” (2021), [arXiv:2107.13338 \[cond-mat.soft\]](https://arxiv.org/abs/2107.13338).
- [55] R. P. Behringer and B. Chakraborty, *Reports on Progress in Physics* **82**, 012601 (2018).
- [56] E. Brown and H. M. Jaeger, *Reports on Progress in Physics* **77**, 046602 (2014).
- [57] S. Henkes, Y. Fily, and M. C. Marchetti, *Phys. Rev. E* **84**, 040301 (2011).